Experimental investigation on the aft-element flapping of a two-element airfoil at high attack angle

Tan Guang-kun*, Shen Gong-xin†, Su Wen-han‡
Beijing University of Aeronautics and Astronautics (BUAA), Beijing, 100083, China

Employing the hydrogen bubble flow visualization and the quantitative PIV measurement, this paper has investigated the structure and evolution of flow around a two-element airfoil at high attack angle when the aft-element was flapping. The experiments had been conducted in the 1.0mx1.2m water channel of BUAA and the experimental Re number based on the chord length was 9000. The results from the experiments show that when the whole foil at high attack angle is still the separated vortices produced by the leading edge will shed off and move downstream apart from leeside zone and the large separation zone will come into being in leeside zone. However, when the fore-element is still and the aft-element is flapping with sine function the separated leading-edge vortices will move downstream close to the leeside and the former large separation zone will remarkably shrink, even disappear, which implies the enhancement of lift and the increase of lift-drag ratio. Furthermore, the influences from the aft-element flapping frequency and amplitude also have been discussed in detail.

Nomenclature

c	=	chord length of the whole foil
f	=	flapping frequency of the aft-element
t	=	flapping time of the aft-element
T	=	flapping period of the aft-element; 1/f
α	=	angle of attack; deg
θ	=	offset angle of the aft-element to chord of the fore-element
θ_0	=	flapping angle amplitude of the aft-element
AE	=	aft-element
FE	=	fore-element
LE	=	leading-edge
TE	=	trailing-edge

I. Introduction

IN a 2-dimensional low speed viscous flow, when an airfoil such as NACA0012 is at a high angle of attack, a flow separation zone comes into being in leeside zone of the airfoil because of converse pressure near the trailing edge. When the angle of attack reaches and surpasses the stall angle of attack the whole airfoil falls into the complete stall mode. At that moment, lift coefficient and life-drag ratio rapidly decline. In order to yield a higher stall angle of attack and greater lift coefficient, in recent years some researchers had investigated many unsteady methods that control flow to improve airfoil's lift character, for example mimic insect flapping wing[1], oscillating wing[2], circulation control[3], sound excitation[4], unsteady heating or cooling[5] etc. Wu[6] had put forward a preliminary thought that employing unsteady airfoil's flap to control vortex flow for enhancing vortices strength generated from the TE, which may be induce stronger vortices in leeside zone and improve lift character of airfoils. Herein, this paper has investigated the structure and evolution of flow around a two-element airfoil at several high attack angles when FE was still and AE was flapping, which resembled Wu's thought, by using the hydrogen bubble flow visualization and the quantitative PIV measurement.

* Dr., Institute of Fluid Mechanics, School of Aeronautics Science and Engineering. tgkpatton@ase.buaa.edu.cn
† Prof., Institute of Fluid Mechanics, School of Aeronautics Science and Engineering. gx_shen05@yahoo.com
‡ Prof., Institute of Fluid Mechanics, School of Aeronautics Science and Engineering. wenhansu@sina.com

II. Experimental model and apparatus

The two-element airfoil with the profile of NACA0012 is shown as Fig.1. The total chord length of the airfoil was 150mm and the FE to the AE ratio was 2:1. The span length was 700mm and the aspect ratio was about 4.7. Both tips of the airfoil were supported by two plexiglass flat plates to eliminate the end effect as shown in Fig.2. Thus the experimental cases in this paper are looked upon as the 2-dimensional flow. The AE were driven by a direct current servo motor and could be flap around the TE of the FE. In Fig.3 the angle of attack between the chord of FE and uniform flow is defined as α, which plays a key role in the flow structure and evolution when the AE is flapping. In all experimental cases, the AE flapped with the sine function $\theta=\theta_0\sin(2\pi ft)$ in which θ denotes the offset angle of the AE to the chord of the FE, that is the flapping central line, θ_0 denotes the flapping amplitude, f is the flapping frequency and t is the flapping time. Ref. 7 has the details about the experimental model. The experiments had been conducted in the 1.0mx1.2m water channel of BUAA and there were triple chord length from the airfoil to the water surface and the bottom. The hydrogen bubble flow visualization had mainly been employed. The platinum wire was fixed before the LE of the FE, normal to the uniform flow and the spanwise, to visualize the flow structure above the leeside and in the wake. The uniform flow was 0.06m/s and the experimental Re number based on the total chord length was 9000.

III. Experimental Results and Analysis

When the two-element airfoil is been placed windward in the uniform flow, If α is set as 0^0 and the AE is flapping, so-called "reverse Karman Vortex Street" will be produced in wake whose formation and dynamic effect are reverse to the traditional "Karman Vortex Street" after a cylinder.

If α is set as 20^0, which is in case of high angle of attack, and the AE is still at the central line of the FE, the separated flow comes into being in the leeside zone, as shown in Fig.4(a). Both from the LE of the FE and the TE of the AE the vortices periodically generate, shed off into wake with the same rotation direction as the case of Karman Vortex Street and move downstream apart from leeside zone. After the AE starts up to flap downwards with the case of $\theta_0=30^0$ and f=0.5Hz, Fig.4(b)-(f) show the evolution of the flow structure around the airfoil. The corresponding St number is about 0.42.

When the AE reaches the lower extreme spot for the first time as shown in Fig.4(b), an obvious counterclockwise rotation vortex T_{ccw1}(the subscript number denotes the flapping cycle of the vortex generation) is produced by the TE and is attaching the AE without shedding off. Fig.4(c) shows the AE returning to the flapping central line at t=0.5T. Because of gradually developing and strengthening, T_{ccw1} has already shed into the wake. At the same time the LE produces a clockwise rotation vortex L_{cw1} responding to the T_{ccw1}. In the course of sequent half flapping cycle, t=0.5T-T as shown from Fig.4(c) to Fig.4(d), the second counterclockwise rotation vortex T_{ccw2} generates and sheds off at the central line whenas the L_{cw1} has fully developed, subsequently shed off and moved downstream along the leeside of the airfoil, which results in the separation zone remarkably shrinking.

When the AE completes one flapping cycle, it starts to steadily flap. Hereafter, at every flapping cycle in the course of returning at the upper extreme spot, the TE always generates a counterclockwise

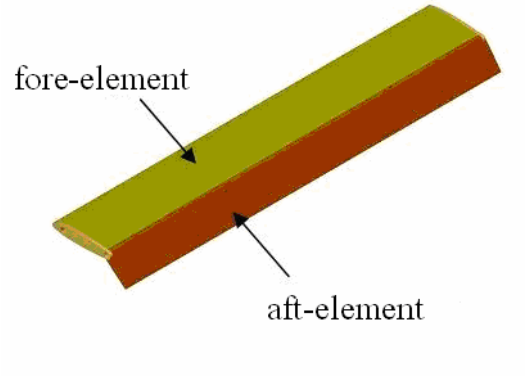

Figure 1. Experimental model: two-element airfoil

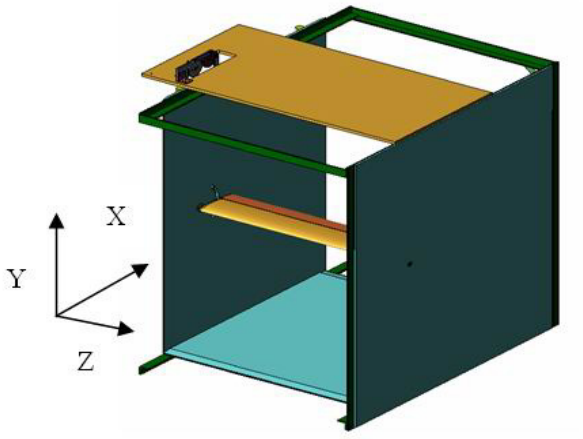

Figure 2. The supporting framework

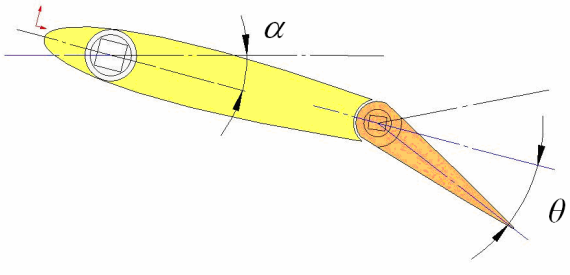

Figure 3. The definition of flapping parameters

rotation vortices, for example T_{ccw3} as shown in Fig.4(e); however, in the course of returning at the lower extreme spot, no obvious vortices come into being, as shown in Fig.4(f). While the AE is steadily flapping, the LE also continuously generates clockwise rotation vortices, for example L_{cw2}, L_{cw3} in Fig.4(e) and L_{cw4} in Fig.4(f), the generation frequency of which equals to the flapping frequency. In Fig.4(e), the third flapping cycle is completed and the AE is flapping downward at the central line. It can be seen that the previous separation zone has disappeared and a series of unsteady vortices are close to the leeside of the airfoil: the LE vortices L_{cw2} and L_{cw3}, and the TE vortex T_{ccw3}. Due to the roll-up effect of L_{cw2} and L_{cw3} moving downstream along the leeside, the flow previously outside the separation zone now can flow into the separation zone, which results in reattachment of the flow above the leeside.

In order to get further validation on this flow phenomenon, a preliminary quantitative PIV measurement had been employed under the same experimental condition including the uniform flow and all flapping parameters. The PIV camera was digital MegaPlus II 2093 made by RedLake with the resolution of 1920*1080 and the straddling time being set as 6ms. The PIV measuring frequency was eight vector fields per flapping cycle and in total 40 flapping cycles had been measured in the phase-locked condition. All the results had be averaged and the velocity contours of the flow with the AE both still and steady flapping are shown in Fig.5. From the comparison of these two cases, It can be clearly found that when the AE is still there is a large separation zone in the leeside zone, but when the AE is steadily flapping the separation zone disappears and a time-averaged flow instead is close to the leeside. Thus, we can daringly anticipate that the AE flapping is most likely to enhance averaged lift coefficient and lift-drag ratio.

This flow phenomenon can be explained by the theory of vorticity conservation. When the AE is still, the vortices generated from the separated shear layer of the LE can't affect the flow in the separation zone; however, when the AE is steadily flapping, the TE of the AE can continuously produce stronger counterclockwise vortices in the course of returning at the upper extreme spot, which incur stronger clockwise vortices from the LE of the FE to reach equilibrium. These powerful LE vortices along with the leeside can roll up the outside flow into the separation zone and as a result change the flow structure in the separation zone and make the flow reattachment onto the leeside of the airfoil. From the view point of flow control, the AE flapping can produce a downstream jet in the separation zone, which resembles the chordwise blowing in the leeside of the airfoil.

There are several influencing factors to affect or control the flow structure above the leeside of the airfoil by flapping the AE. Firstly the influence from the attack angle of the FE, that is α, is taken into consideration due to it directly determines the generation of the separation zone. With the same cases of the uniform flow and the flapping parameters of the AE, four different cases of α, 10^0, 20^0, 30^0 and 40^0, are compared in the flow visualization as shown in Fig. 6. In these figures, the left column is before the start-up of the flap and the right is at the moment that the AE is steadily flapping downwards and just reaches the flapping central line. From the left column in Fig.6 it can be found that with α increasing from 10^0 to 40^0, the slope angle of the separated shear layer relative to the uniform flow is increasing and the domain of the separation zone is also gradually expanding. Regarding every case of α, comparing the left figures (AE still) and the right ones (AE flapping) can find that the slope angle of the shear layer decreases after the AE starts up and in the shear layer several obvious clockwise vortices are produced and the separation zone is shrunk. From the right column in Fig.6 we can also see that with the flapping parameters of the AE unchanged, the increase of α will result in the enlargement of the separation zone and the dimensions of the LE vortices become larger but their strength weaker. Moreover, the LE vortices will not move down along with the leeside but along with the boundary of the separation zone and break away the leeside, as shown in Fig.6(c)(d). Therefore the roll-up effect of outside flow flowing into the separation zone is worsened, which makes it more difficult to change the flow structure of the separation zone. Thus it can be summarized that when α of the FE is less than 20^0, the AE flapping can incur the obvious flow reattachment onto the leeside of the foil and the shrinking of the separation zone, even disappearance; however, with α increasing, for example be greater than 30^0 or 40^0, the effect of flow reattachment is not good due to the enlargement of the separation zone and the weakening of the influence of the LE vortices.

From the above-motioned analysis, we can see that in order to enhance the influence of the LE vortices on the separation zone and make the flow reattachment it needs to increase the strength of the LE vortices which are indirectly induced by the AE flapping. Therefore to control the AE flapping parameters is an effective method to change the strength of the LE vortices. The comparison of the flow structures with the cases of the AE flapping frequency f=0.5Hz, 0.667Hz and 1Hz is shown as Fig.7, in which α of the FE is 30^0 and the AE is flapping downwards at the central line. The flapping amplitude θ_0 is 15^0 in the left column and 30^0 in the right column. From Fig.7 it can be found that although there is always a large separation zone above the leeside of the airfoil, with f increasing, (1) the generation frequency of the LE vortices is also increasing, which means during a unit time more LE vortices will generate; (2) the TE vortices are more obvious and powerful, which can induce more powerful LE vortices. Because of these two points, the induced total vorticity from the LE, that is the vorticity of every LE vortex multiply the number of the LE vortices, is also increasing. Furthermore, the increase of θ_0 of the AE flapping can't change the generation frequency of the LE vortices but can enhance the

strength of every LE vortex. Thus, increasing the flapping amplitude θ_0 of the AE is also beneficial for outside flow to roll up into the separation zone and consequently shrink its domain.

IV. Conclusions

From the experimental results and the above-mentioned analysis, the following conclusions can be summarized:

1. For two-element airfoil that consists of a fore-element and an aft-element in tandem, when the fore-element is at a higher angle of attack (mostly $\alpha \leq 30^0$) and the aft-element is flapping, it can generate powerful separated vortices from the leading-edge of the fore-element. These vortices will roll up outside flow into the separation zone and as a result shrink the domain of the separation zone.
2. In the same cases of uniform flow and the flapping parameters of the aft-element, the lower the attack angle of the fore-element is, the more obviously the flapping aft-element shrink the separation domain, even make it disappear and flow reattach, and vice versa.
3. The frequency of generation and strengthen of the separated vortices generated from the leading-edge are under the control of the flapping frequency and amplitude: the frequency of generation equals to the flapping frequency; the greater the frequency or the amplitude is, the larger and the stronger vortices generate, and vice versa.
4. The flap of the aft-element is greatly likely to improve the averaged lift coefficient and the lift-drag ratio of the whole airfoil but it should be further confirmed.

References

[1]Sun, M., "Unsteady lift mechanisms in insect flight" (in Chinese), *Advances in Mechanics*, Vol.32, No.3, 2002, pp. 425-434.

[2]Carr, L. W., "Progress in analysis and prediction of dynamic stall", *J. Aircraft*, No. 25, 1988, pp. 6-7.

[3]Nielson, N. J., Biggers, J. C., "Resent progress in circulation control aerodynamics", *AIAA-87-0001*, 1987.

[4]Ahuja, K. K., Whipkey, R. R., Jones, G. S., "Control of turbulent boundary layer flows by sound", *AIAA-83-0726*, 1983.

[5]Wu, J. Z., Vakili, A. D., Wu, J. M., "Review of the physics of enhancing vortex lift by unsteady excitation", *Prog. Aerospace Sci.* No. 28, 1991, pp. 73-131.

[6]Wu, J. M., "The dawn of aerodynamics" (in Chinese), *International Aviation*, No. 8, 1985, pp. 2-7.

[7]Tan, G. K., Shen, G. X., "Flow visualization of 2-freedom oscillation of airfoil", *The Seventh Triennial International Symposium on Fluid, Control, Measurement and Visualization (FLUCOME'03)*, Sorrento in Italy, 2003, pp. 262.

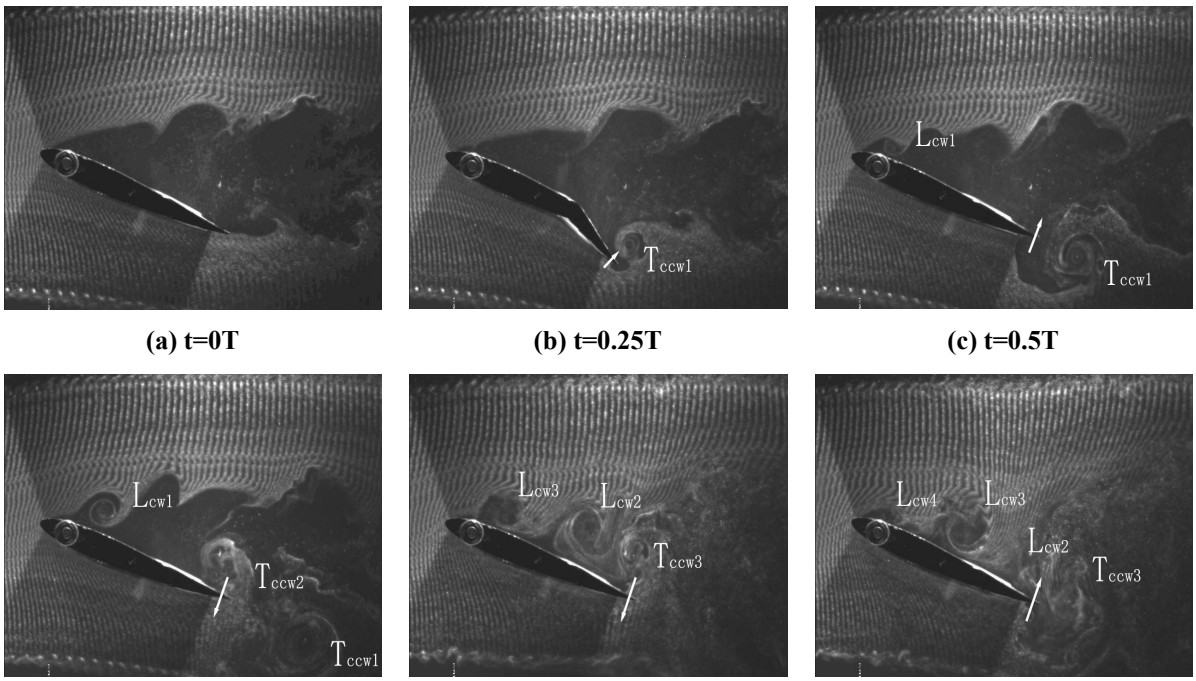

(a) t=0T **(b) t=0.25T** **(c) t=0.5T**

(d) t=1T **(e) t=3T** **(f) t=3.5T**

Figure 4. The evolvement of flow structure after the aft-element start-up. α=20^0, θ_0=30^0 and f=0.5Hz.

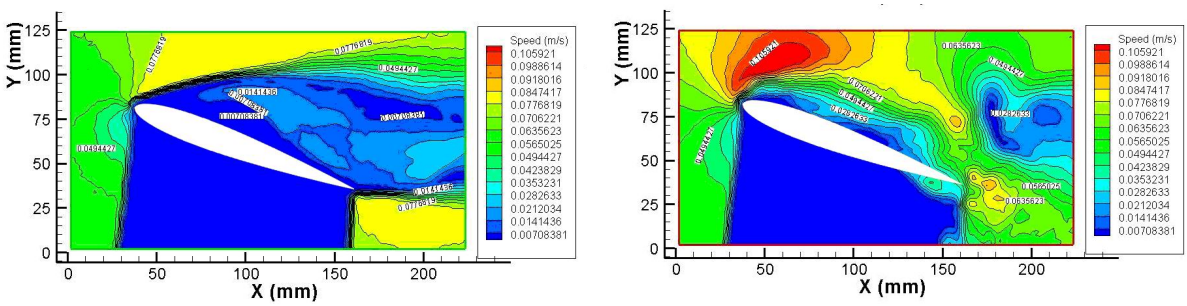

Figure 5. The time-averaged velocity contours based on PIV measurement about the evolvement of flow structure after the aft-element start-up, left: before the aft-element start-up, right: with the aft-element steadily flapping. α=20^0, θ_0=30^0 and f=0.5Hz.

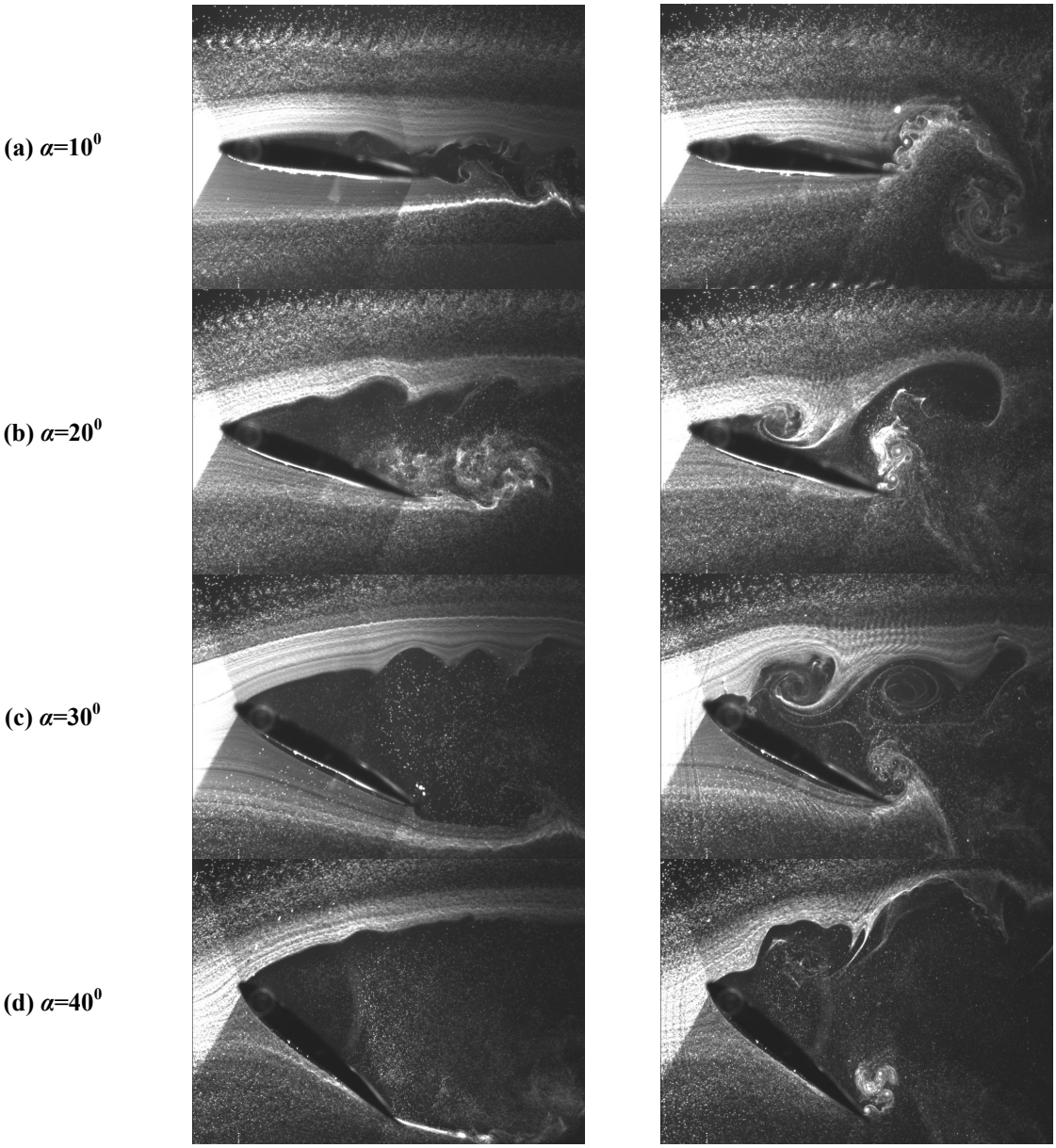

Figure 6. The evolvement of flow structure at different angle of attack after the aft-element starts-up. θ_0=30^0, f=0.5Hz

(a) f=0.5Hz

(b) f=0.667Hz

(c) f=1Hz

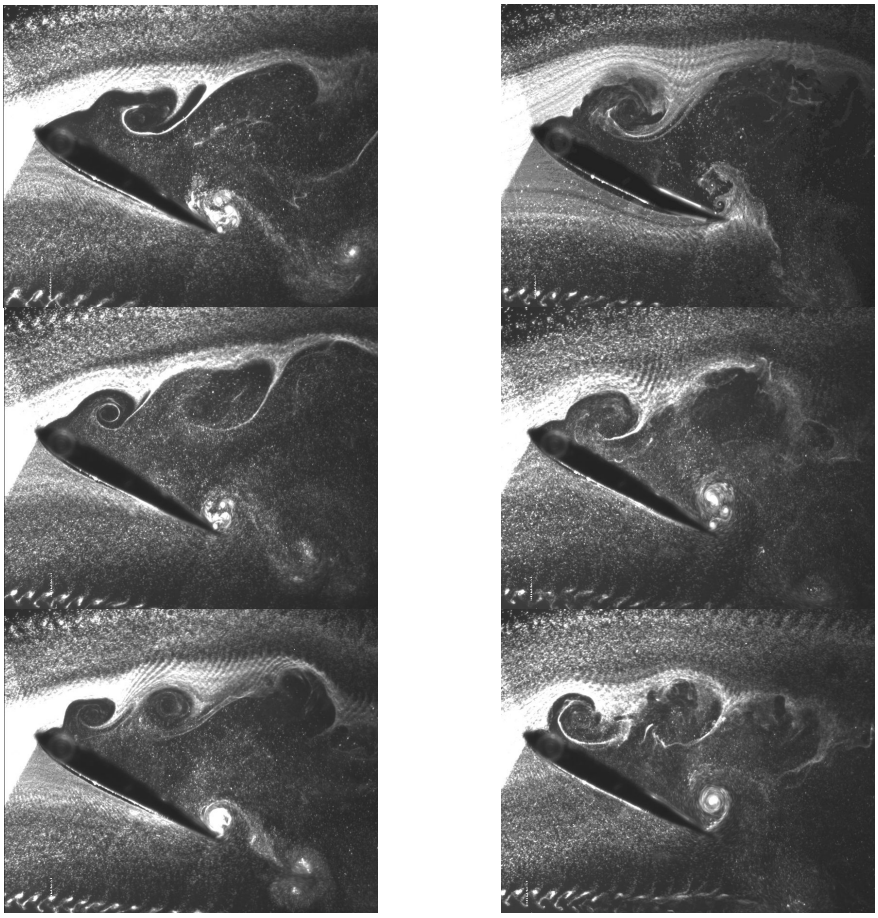

Figure 7. The evolvement of flow structure at different frequency and amplitude. α =30^0, left: θ_0=15^0, right: θ_0=30^0